Round-robin measurements of the laser induced damage threshold with sub-picosecond pulses on optical monolayers

L. Lamaignère, [1] A. Ollé, [1] M. Chorel, [1] N. Roquin, [1]
A. A. Kozlov,[2] B. N. Hoffman,[2] J. B. Oliver,[2] S. G. Demos[2],
L. Gallais[3]
R. A. Negres[4]
A. Melninkaitis[5]

[1]CEA, CESTA, F-33116 Le Barp, France
[2]Laboratory for Laser Energetics, University of Rochester, 250 E. River Road, Rochester, New York 14623-1299, USA
[3]Aix-Marseille University, CNRS, Centrale Marseille, Institut Fresnel, 13013 Marseille, France
[4]NIF and Photon Sciences, Lawrence Livermore National Laboratory, 7000 East Avenue, Livermore, CA, USA
[5]Vilnius University, Laser Research Center, Saulėtekio ave. 10, LT-10223 Vilnius, Lithuania

Abstract: The standardization and comparison of laser-damage protocols and results are essential prerequisites for development and quality control of large optical components used in high-power laser facilities. To this end, the laser-induced–damage thresholds of two different coatings were measured at five well equipped laboratories involved in a round-robin experiment. Tests were conducted at 1 μm in the sub picosecond range with different configurations in terms of polarization, angle of incidence, and environment (air versus vacuum). In this temporal regime, the damage threshold is known to be deterministic, i.e., the continuous probability distribution transitions from 0 to 1 over a very narrow fluence range. This in turn implies that the damage threshold can be measured very precisely. These characteristics enable direct comparison of damage-threshold measurements between different facilities, with the difference in the measured values indicating systematic errors or other parameters that were not previously appreciated. The results of this work illustrate the challenges associated with accurately determining the damage threshold in the short-pulse regime. Specifically, the results of this round-robin damage-testing effort exhibited significant differences between facilities. The factors to be taken into account when comparing the results obtained with different test facilities are discussed: temporal and spatial profiles, environment, damage detection, sample homogeneity and nonlinear beam propagation.

I. INTRODUCTION

The increase in energy and/or power of short-pulse–class lasers (OMEGA-EP [1], PETAL [2], ARC [3]) in the picosecond regime requires components always more resistant to laser intensities, whether these are the compression gratings [4] or the mirrors that transport the beams to the target [5, 6]. As a result, dedicated damage-testing facilities have been developed to provide an accurate determination of a component's ability to withstand the operational laser fluence. The question of the representativeness of the laboratory measurement arises logically in relation to the behavior of the components in real operational conditions. The environmental conditions are often not exactly the same, while the characteristics of the beams are somewhat different. But before even dealing with the representativeness of the measurement, it is just as relevant to question the reproducibility of tests carried out on different set-ups. Reproducibility in this instance is based on comparing measurements performed according to nominally the same protocol but on different facilities. *De facto*, the latter can differ in many respects, the characteristics of the laser beams are unavoidably not identical, and the diagnostics used for performing metrology are also different. Finally, the environmental conditions can also vary, and, in the end, the data processing may likewise prove to have some influence on the results to be compared. It is therefore important to consider that these differences can give rise to variations in the experimental results obtained on the different installations.

In the pulse regime reported in this work (subpicosecond), it is well documented that the damage threshold for dielectric materials in pristine areas (free from obvious defects such as micro-scale coating defects) is deterministic. This is reported in several previous works [7, 8, 9, 10]. This is characterized by

a very definite threshold behavior (deterministic), namely that below a threshold value of energy density, the components are resistant to the laser flux, while above the threshold the damage is certain. This threshold can then be determined with great precision and this behavior is well suited to the aim of this study, i.e. comparison of results obtained from different laboratories. Damage is associated with electronic processes, and it is closely linked to the properties of materials, in particular their optical band gap and defect concentration. It turns out therefore that the damage threshold can even be predicted theoretically knowing the properties of the materials and those of the laser pulse [11, 12, 13].

The objective of the work reported herein consisted of comparing results of Laser-Induced-Damage-Threshold (LIDT) on two dielectric materials (HfO_2 and SiO_2) in the form of monolayers tested on five different laser facilities. The latter have very similar characteristics such as similar wavelengths (around 1 μm), pulse duration (0.8 ps), and beam size. The tests were carried out according to an identical protocol described by the ISO standard [14]. After the presentation of the raw results of LIDT measurements obtained using the various installations, the second part of the article endeavors to identify and then analyze the various parameters which are hypothesized to be the sources for the observed discrepancies between these measurements.

II. RESULTS

II.1 Materials

Hafnia (HfO_2) and silica (SiO_2) monolayers have been selected for these tests as they are common materials used in multilayer dielectric optical components employed in short-pulse laser systems as high- and low-refractive-index materials, respectively. They have been deposited by electron-beam evaporation with ion assistance (IAD) on BK7 substrates. The layer thicknesses are 149.9 and 194.3 nm, respectively, with refractive indices of 1.930 and 1.448 determined at 1053nm via ellipsometry. Multiple samples from the same deposition batch were fabricated and sent individually to the five testing facilities. This means that each test was carried out on a single sample which is nominally identical to all other samples in the batch.

II.2 Experimental conditions

The experimental conditions have been selected to be as close as possible for the different set-ups:

- Wavelength around 1 μm: 1053 or 1030 nm as a function of the laser source.
- Pulselength: around 800 fs. This value being quite common to the different lasers.
- Environment: in air due to the fact that only two set-ups are equipped with a vacuum chamber. Some tests have also been performed in a vacuum environment for comparison.
- Angle of incidence (AOI): 0 and 45°.
- Polarization: P and S polarizations.

The four testing configurations (0°-P_{pol} ; 45°-P_{pol} ; 0°-S_{pol} ; 45°-S_{pol}) were implemented using the ISO 1-on-1 procedure on each set-up [14]. Because damage in the sub-picosecond regime is deterministic, there is no need to perform a detailed statistical analysis by reproducing the measurement on a large number of spots *per* fluence. The reported experimental LIDT ($LIDT_{exp}$) is defined as the mean between the lowest fluence where damage is detected and the highest fluence where no damage occurs. The uncertainty of the measurement is set to be the mean absolute deviation between these two fluences. Therefore, the uncertainty of the measurement can be reduced by testing additional fluences around the damage-threshold fluence.

The spatial profile of the laser-beam intensity was nearly Gaussian for all lasers used in this study. The equivalent areas are in the range [0.4×10^{-4} – 3.5×10^{-4} cm²] which corresponds to beam diameters in the range [70 – 210 μm]. The *in situ* damage detection was done either a) analyzing the variation of the scattered light from the focal spot (damage is recorded when the scattered light increases, based on Schlieren imaging), or b) direct imaging using a long-working distance microscope. However, these *in situ* detection approaches were used only for guidance during the 1-on-1 procedure and not as a damage threshold determination. The final determination was a precise observation with a differential-interferential–contrast (DIC) microscope, as recommended by the ISO standard. A damage site is

defined as a modification, e.g. pits or discoloration, on the sample seen by means of the DIC. The results reported in this manuscript obtained from different facilities are presented anonymously in the form Lab A, B, C, D, E (for laboratory A, B, C, D, E).

	Lab A	Lab B	Lab C	Lab D	Lab E
Beam diameter @ 1/e (μm)	73 ± 17	173 ± 25	210 ± 10	100 ± 1	186 ± 14
Beam area @ 1/e (cm^2)	(4.20 ± 0.22) $x10^{-5}$	(2.36 ± 0.05) $x10^{-4}$	(3.48 ± 0.01) $x10^{-4}$	(7.85 ± 0.01) $x10^{-5}$	(2.73 ± 0.02) $x10^{-4}$
Spatial profile	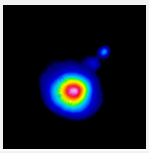	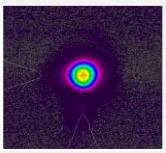	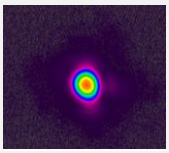	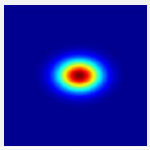	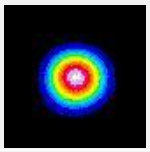
Fluence determination	Maximum fluence of beam profile	Maximum fluence of beam profile	Maximum fluence of beam profile	Maximum fluence of beam profile	Maximum fluence of beam profile

Table 1: Beam sizes and spatial profiles.

II.3 Experimental laser-induced damage threshold ($LIDT_{exp}$)

The experimental results of LIDTs obtained by the five laboratories on the two monolayers and for the four configurations are reported in Table 2. They are expressed in energy density (fluence in $J.cm^{-2}$), and reported based on the beam normal, that is to say that the beam area on the layers is not corrected for the angle of incidence. The LIDTs are raw, as-measured data without taking into account the electric field intensity inside the monolayer, which is different for each configuration. For illustration purposes, Fig.1 shows two representative damage sites on HfO_2 irradiated at 10% and 20% above damage threshold, respectively, with the former being a light discoloration while the latter is a pit.

	SiO_2 monolayer				HfO_2 monolayer			
	P-pol		S-pol		P-pol		S-pol	
	0°	45°	0°	45°	0°	45°	0°	45°
Lab A	4.15	5.07	-	5.11	3.40	4.67	-	5.24
Lab B	4.23	Out of range	4.42	Out of range	3.90	4.44	3.98	Out of range
Lab C (air)	2.86	3.81	2.87	3.73	2.82	3.24	2.59	3.65
Lab C (vacuum)	3.44	4.18	3.09	4.77	3.19	3.83	2.85	4.35
Lab D	2.90	3.86	-	3.92	2.98	3.30	-	4.31
Lab E (air)	-	-	-	-	3.00	3.50	-	3.99
Lab E (vacuum)	-	-	-	-	-	4.25	-	4.75

Table 2: Experimental LIDTs ($LIDT_{exp}$) measured by the five laboratories (labeled as Lab A, Lab B, Lab C, Lab D, Lab E) on the two dielectric monolayers (SiO_2 and HfO_2). All values represent beam normal fluences in $J.cm^{-2}$. Results are also reported by lab C and lab E in a vacuum environment. 'Out of range' means that fluences necessary to perform the test cannot be reached. '-' means that the test was not realized.

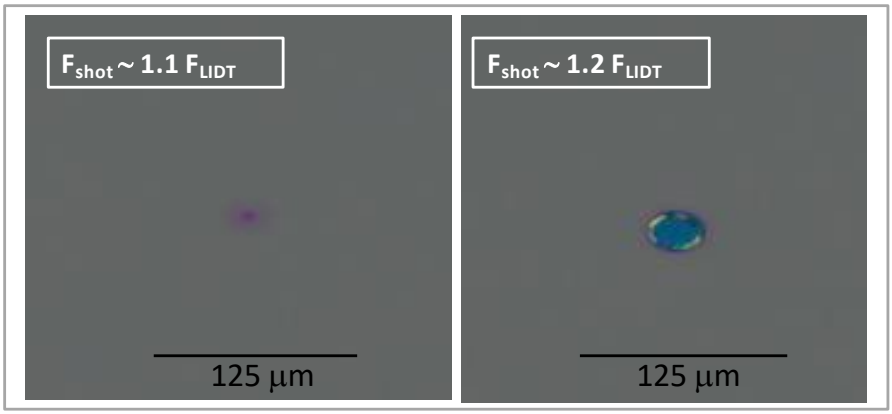

Figure 1: post-mortem observation by means of Nomarski microscope for two irradiations on HfO_2 at 10 and 20% above experimental $LIDT_{exp}$.

III. DISCUSSION

III.1 Electric Field Intensity (EFI)

We base our discussion on the first order assumption that each dielectric material is characterized by its own damage threshold. It is a property which is specific to it as well as other properties such as the melting temperature, the conductivity, the permittivity, etc. A material is thus characterized by its intrinsic laser-induced damage threshold ($LIDT_{int}$), a property of the material independent of experimental conditions such as the angle of incidence and the state of polarization of the beam. These last two parameters act on the maximum value of the electric field intensity (EFI) and on its position within the material (see figure 2). Thus intrinsic threshold and experimental threshold for a given layer are related by the EFI via the relationship:

$$LIDT_{int} = LIDT_{exp} \times EFI_{max} \quad (1)$$

Finally, it also means that whatever the experimental conditions (AOI and polarization states), the $LIDT_{int}$ must be the same despite different $LIDT_{exp}$. This property is beneficial and more essential to the damage metrology because it makes it possible:

- To compare results obtained under different experimental conditions.
- To check on the repeatability of a measurement on the same installation.
- To validate the accuracy of a measurement under uncertain experimental conditions, such as the occurrence of nonlinear effects (see for instance Section III.2).

Values of the refractive index and thickness were used to calculate numerically the electric-field–intensity distribution within each monolayer using OptiLayer software. Samples are modeled as a monolayer deposited on a semi-infinite BK7 substrate and a superstrate with a refractive index of 1 (air or vacuum). Samples are illuminated at normal incidence, or 45°AOI, from the incident medium with a linearly polarized plane wave (horizontally or vertically) at the wavelength λ = 1053 nm. The distribution of the square of the time-averaged electric field $|E|^2$ is calculated and normalized by the incident electric field $|E_{inc}|^2$. The maximum enhancement of the electric-field intensity in the layer, $|E|^2/|E_{inc}|^2$ denoted by EFI_{max} is estimated and reported in Table 3 for the four configurations and the two monolayers.

$$EFI = \left|\frac{E}{E_{inc}}\right|^2 \quad (2)$$

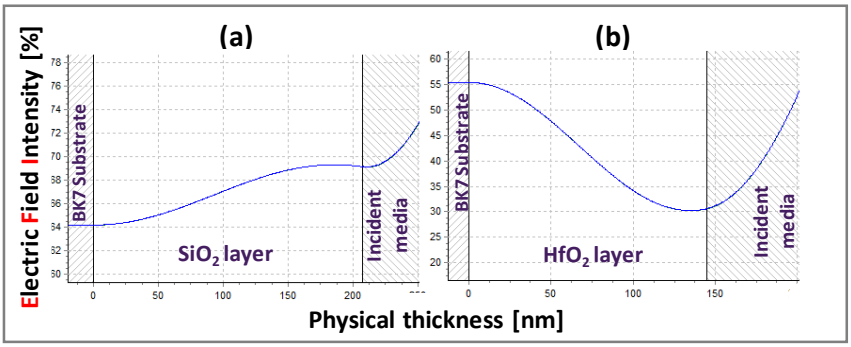

Figure 2: Electric Field calculations in SiO_2 (a) and HfO_2 (b) monolayers at 0° of AOI, P or S polarizations. The EFI is maximum (69.9%) at the top of the silica layer (at the air interface) and maximum (54.6%) at the bottom of the hafnia layer (at the substrate interface).

	P-pol		S-pol	
	0°	45°	0°	45°
SiO_2: EFI_{max}	0.699	0.565	0.699	0.549
HfO_2: EFI_{max}	0.546	0.422	0.546	0.372

Table 3: Calculated EFI_{max} in SiO_2 and HfO_2 monolayers at 0 and 45° in P and S polarizations.

III.2 Intrinsic laser-induced damage threshold ($LIDT_{int}$)

The intrinsic LIDT ($LIDT_{int}$) for the two monolayers was estimated from eq. (1) using the $LIDT_{exp}$ values provided in table 2 and calculated EFI_{max} reported in table 3. Results are given in tables 4 and 5 for SiO_2 and HfO_2 monolayers, respectively. For a meaningful comparison, only results obtained in air environment are reported. The last three columns of the tables indicate the average fluences measured on each installation as well as the standard deviation on the measurement. The standard deviation is a qualitative indicator of the repeatability of the measurement. The last line corresponds to the average of the measurements made on each installation.

	SiO_2 monolayer						
	P-pol		S-pol		$LIDT_{int}$		
	0°	45°	0°	45°	mean	σ	σ/mean
Lab A	3.03	2.99	-	2.93	2.99	0.03	0,010
Lab B	2.96	Out of range	3,09	Out of range	3.02	0.07	0.023
Lab C	2.00	2.15	2.01	2.05	2.05	0.04	0.019
Lab D	2.03	2.18	-	2.15	2.12	0.05	0.023
mean					2.55	0.53	0.209

Table 4: Intrinsic LIDTs ($LIDT_{int}$) of SiO_2 monolayer estimated by means of relation (1) from experimental data of table 2 and EFI_{max} of table 3. Thresholds are given in terms of energy density (fluence) in $J.cm^{-2}$.

	HfO_2 monolayer						
	P-pol		S-pol		$LIDT_{int}$		
	0°	45°	0°	45°	mean	σ	σ/mean
Lab A	1.94	2.06	-	2.04	2.01	0.04	0.020
Lab B	2.13	1.87	2.17	Out of range	2.06	0.09	0.044
Lab C	1.54	1;37	1.41	1.36	1.42	0.04	0.028
Lab D	1.63	1.39	-	1.6	1.54	0.07	0.045
Lab E	1.64	1.48	-	1.48	1.53	0.09	0.059
mean					1.71	0.30	0.175

Table 5: intrinsic LIDTs ($LIDT_{int}$) of HfO_2 monolayer estimated by means of relation (1) from experimental data of table 2 and EFI_{max} of table 3. Thresholds are given in terms of energy density (fluence) in $J.cm^{-2}$.

To better visualize the distribution of the LIDT values obtained from measurements in the 5 different facilities, the results are also presented in the form of a histogram (figure 3). To quantify this distribution, the ratio between standard deviation and mean (σ/mean) is used to estimate the deviation of the measurement. A number of behaviors can be readily appreciated:

- Globally, data are significantly dispersed (Figure 3).
- Within each lab, the repeatability is about a few percent (lower than 7.5%, last column of tables 4 and 5).
- The reproducibility (agreement between the results of measurements of the same measurand in the same configuration carried out with the same methodology between the 5 laboratories) is around 21% (last cell in tables 4 and 5). This value is very large even if the error budgets of each installation are not taken into account at first analysis. Given that the experimental conditions are very similar and the fact that particular attention was paid to metrology during these tests to accurately determine the onset of damage, this difference between the LIDT maximum and minimum values (38%) is absolutely unexpected and highly undesirable. We will attempt in the next sections to provide insight into the possible underlying mechanisms.

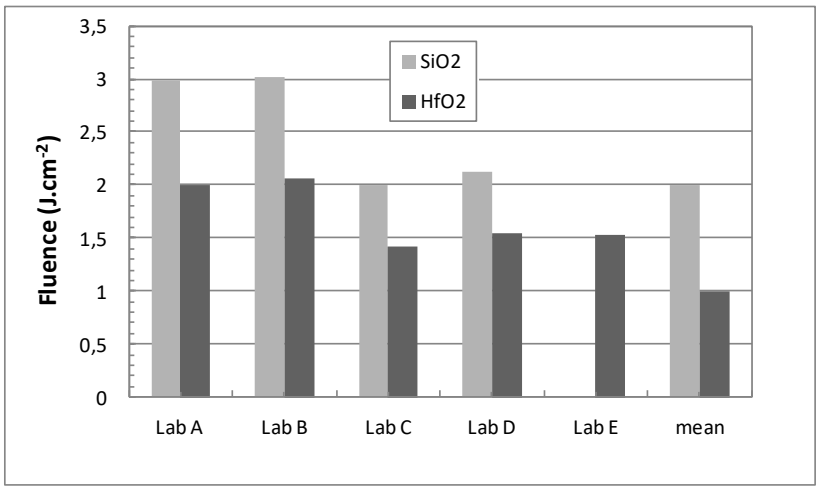

Figure 3: Histogram of intrinsic LIDTs on each laboratory for SiO_2 and HfO_2 monolayers. The last two bars correspond to the averages of the different installations.

III.2 Characteristics of the laser pulses

The tests were carried out at a pulse duration (τ) of 800 fs in order to achieve nominally identical conditions at the five laboratories regarding this parameter. The small deviations in this value were corrected using the temporal scaling law reported by Mero [8], in the form of $F_{th} \sim \tau^{\kappa}$ with an exponent κ of about 0.30 and 0.33 for hafnia and silica, respectively. F_{th} stands for Laser-Induced–Damage threshold, the LIDT acronym in this paper.

The pulse durations in all cases were estimated from the autocorrelation trace of an autocorrelator, but that estimation strongly depends on the assumption made on the shape of the temporal pulse (Gaussian, hyperbolic secant, Lorentzian). An uncertainty up to 10% on this measurement has to be considered. On the other hand, the exact intensity profile must also be considered. Recently, Ollé [13] has reported experimentally and numerically large LIDT differences due to small differences in relatively similar intensity profiles (see figure 15 of [13]). Ideally, exact temporal profiles have to be determined by means of specific apparatus like Frequency-Resolved Optical Gating (FROG) [15], SPIRITED [16], or other equivalent diagnostics. Finally, LIDT errors due to the pulse duration are certainly at least of the order of 5% but can also reach 30% for different intensity profiles. For this, we refer to section III of Ollé's article [13] dealing with the influence of temporal shape on the temporal scaling law.
Numerical $LIDT_{int}$ estimations based on the model described in [13] were also performed for 3 different temporal profiles acquired during this campaign at Lab B, by means of SPIRITED diagnostic. Small differences appear on their shapes and their FWHM pulse durations are close (Full Width Half

Maximum: 782 – 801 – 810 fs), see Fig. 4. The table 6 reports the $LIDT_{int}$ numerical estimations for SiO_2 and HfO_2. Deviations between maximum and minimum values are about 9 and 5% for SiO_2 and HfO_2, respectively. These deviations are part of the repeatability of the measurement on the same set-up.

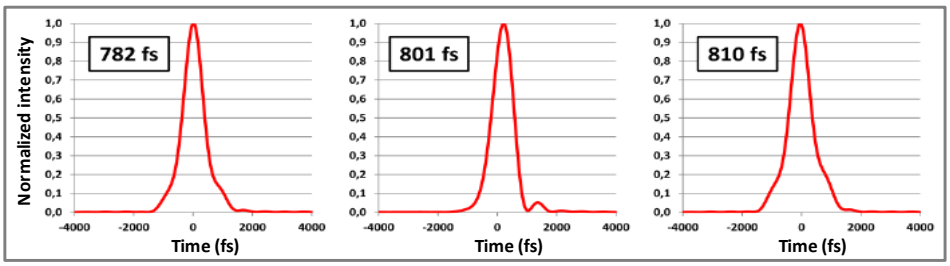

Figure 4: Three different temporal profiles measured during the campaign at Lab B by means of SPIRITED diagnostic, for the same laser fluence.

	Pulse duration (fs)			mean	σ	σ / mean	(max-min)/σ
	782	801	810				
SiO_2	4.94	4.67	5.11	4.91	0.22	0.05	0.09
HfO_2	4.47	4.36	4.59	4.47	0.12	0.03	0.05

Table 6: numerical LIDTs of SiO_2 and HfO_2 monolayers estimated from numerical model for the 3 temporal profiles given in figure 4. Relation (1) can be applied to estimate the intrinsic LIDT.

Another parameter that may have a significant impact is the temporal contrast. Prepulses and/or postpulses can have a double effect. First, it is established that the ablation efficiency in dielectrics depends on the delay between the pre-/post-pulses and the main pulse [17]. The first pulse promote electrons into the conduction band while the second pulse induces the ablation of the dielectric. The analogy with laser damage mechanisms is obvious. These pre- and post-pulses must be minimal and sufficiently spaced in time from the main pulse to avoid any pre- or post-excitation effect. In addition, these pulses are taken into account in the energy balance (the measurement of the pulse energy is integrated on a pyroelectric detector or on a photoelectric cell), biasing the true value of the intensity/energy involved in the process and damage mechanisms by the main pulse. The impact of this parameter is currently not known. Therefore, it may be important to include in the diagnostics the capability to measure the full intensity profile (for that purpose see figure 4 of [13]).

The determination of beam fluence has been the gold standard in damage testing for decades. Its accuracy is intimately linked to a precise and rigorous determination of the equivalent beam area. However, it can be challenging to ensure that the measurement is correct to better than 5% [18], and the measure can strongly diverge via seemingly minor effects. Here we detail a few missteps to be aware of when managing short pulses and small beams.

a) The waist position and length: Lenses with short focal lengths are commonly used on short-pulse damage set-ups in order to focus the laser beam on the sample to be tested and achieve damage threshold fluences. As a result, the Rayleigh length is also very short. The beam area is the same for only a few millimeters [13] and diverges strongly beyond. An approximate positioning of the sample and/or of the measurement camera can lead to a significant error on the beam area.

b) The CCD sensor size / Ratio signal/noise: The pixel size of cameras commonly used to measure the beam profiles is only a few microns in length (~5µm) and they are coded over 12-bit gradation or more. These two characteristics allow a high-quality resolution with corresponding accurate determination of the energy in the wings of the beam and a very good resolution of the maximum intensity of the same beam. However, the sensor size is large, of the order of 8 by 6mm in comparison with the size of the beam (<0.2 mm), that is to say a ratio close to 50. The total number of pixels on these sensors is around 2 million (1600 * 1200) but the number of pixels illuminated for a beam of a hundred microns is only of the order of 2000, in this case a ratio of 1000. Thus, the signal-to-

noise ratio is strongly unfavorable for such small beams with such a large sensor. It is therefore advisable to adjust the size of the sensor to the size of the beam by imposing an adapted ROI (Region Of Interest) around the beam. In addition, cross-analysis between laboratories of the measurement of a given beam size have given a difference of at least 5%.

c) Nonlinear beam propagation: Operating with short pulses can lead to non-linear propagation inside transmissive optical components that are designed to facilitate energy control (waveplate and polarizer), focus the beam on the sample (lens), or split the beam to diagnostics (beamsplitter). This nonlinear propagation can modify the beam profile and its focal position. A beam size variation up to 5% has been reported by changing the pulse duration from 0.8 to 4 ps for a fixed beam energy (see fig. 18 of [13]). This could also be the case with the energy variation.

d) Operational environment: When laser-damage measurements of dielectric components are carried out, many questions arise as to the effect of the environment. This issue is quite complex, and it is not the purpose of this discussion to deal exhaustively with this topic. However, two issues are of particular interest. First, how is the beam propagation in air affected, which can lead to air breakdown? Second, how do the film properties (refractive index, layer thickness etc.) change with the environment, potentially modifying the value of the EFI in the layer?

Self-focusing is known to be an important parameter for the design of short-pulse laser-damage setups, which is why it is recommended to carry out tests under a vacuum environment to circumvent this issue (with the difficulties inherent in measurements in a vacuum chamber). For tests in an air environment, it is necessary to estimate the B-integral through the focal volume prior to the test surface. In the set-ups, B-integral is due to the self focusing in the air after the last focusing lens. For a Gaussian beam with a wavelength λ and waist radius ω, the Rayleigh distance Z_R is defined as:

$$Z_R = \pi \frac{\omega^2}{\lambda} \tag{3}$$

The intensity I at the focal spot is given by the relation:

$$I = \frac{2.E}{\tau \pi \omega^2} \tag{4}$$

Where E is the energy and τ the pulse duration. The B-integral can be estimated by:

$$B = \frac{2\pi}{\lambda} n_2 \int_0^{Z_R} I(z) dz \tag{5}$$

The intensity I is assumed to be constant within the Raleigh distance Z_R, then combination of Eq. (3), (4) and (5) gives:

$$B = \frac{4\pi}{\lambda^2} n_2 \frac{E}{\tau} \tag{6}$$

During all of the tests, samples were tested up to 6 J.cm^{-2} in the beam normal at 800 fs. This fluence was obtained with a maximum energy of 2 mJ. It has been established that the nonlinear refractive index of air was $n_2 = 3.10^{-19}$ cm²/W [19]; it follows that equation (6) gives a B-integral value of B ~ 0.85. This value is below the self-focusing limit which can be taken as B ~ 2 radians [20]. Thus beam propagation should not be subject to self-focusing.

This issue was also verified experimentally by changing the AOI from 0 to 45°and verifying that the intrinsic LIDT ($LIDT_{int}$) estimated from the experimental LIDT ($LIDT_{exp}$) remains constant. This is based on the following testing hypothesis: given that the test fluence increases when the AOI is increased, if the self-focusing effect is negligible one should find the same intrinsic LIDT for any AOI and corresponding fluence. The EFI was calculated at each AOI. Results are given in table 7. Increasing the AOI means an increase of the experimental fluence (from 3.77 to 5.57 J.cm^{-2} in the reported case). And yet, it is observed that the intrinsic LIDT is constant within experimental error. The mean value and the standard deviation are 2.06 and 0.02 J.cm^{-2}, respectively, which is a variation of less than 1%. It can be concluded that:

- The intrinsic LIDT can be determined at any AOI, based on the calculated EFI.
- No self-focusing occurred during these measurements, even at high energy.

	0°	10°	20°	30°	35°	40°	45°
LIDTexp (J.cm^{-2})	3.77 ± 0.07	3.75 ± 0.01	4.15 ± 0.08	4.50 ± 0.06	4.70 ± 0.10	5.08 ± 0.01	5.57 ± 0.01
EFI	0.541	0.533	0.509	0.466	0.438	0.405	0.366
LIDTint (J.cm^{-2})	2.04 ± 0.07	2.00 ± 0.01	2.11 ± 0.08	2.10 ± 0.06	2.06 ± 0.10	2.06 ± 0.01	2.08 ± 0.01

Table 7: intrinsic LIDTs ($LIDT_{int}$) of HfO_2 monolayer estimated from experimental LIDTs ($LIDT_{exp}$) tested in air environment and S-polarization between 0 and 45° AOI during the campaign at Lab B. EFI was determined at each angle.

The question of the impact of the environment for testing is a difficult question. Specifically, can one extrapolate results from thresholds measured in the air to expected thresholds in vacuum? This is a complex question to which an element of an answer is brought indirectly in this paragraph. To explore this question, EFI values were estimated for the layers in vacuum. We start from the principle that the vacuum can be approximated by a dry air environment, in particular with regards to the refractive index of the dielectric layers. The estimation of the refractive index not being possible with our means in vacuum, measurements with a spectrophotometer in dry air were carried out in order to estimate the refractive index of the layers, and therefore determine the value of the EFI. Refractive indices, and consequently EFIs, were found to be little different regardless of the environment. Damage thresholds were subsequently measured in ambient air (45% relative humidity) and in dry air (4% relative humidity) on one hafnia monolayer and one silica monolayer. Experimental LIDTs were also measured to be approximately the same. Finally, intrinsic LIDT values are quite similar (see table 8), with differences of less than 3%. These results suggest that 'intrinsically', environment should have a negligible effect on the damage thresholds of these samples. A key aspect of this determination is the relatively slow change in EFI versus layer thickness for a monolayer, such as those tested in this study, versus the very rapid change in EFI for some multilayer coating designs [21]. The EFI becomes much more complex when these materials are integrated in multilayer coating designs, requiring additional investigation beyond the scope of this work.

Dielectric monolayer	Environment	Refractive index at 1053 nm	Physical thickness of layer (nm)	EFImax	$LIDT_{exp}$ (J.cm^{-2})	$LIDT_{int}$ (J.cm^{-2})
HfO_2	Ambient Air	1.93	149.9	0.5414 ± 0.0160	3.90 ± 0.01	2.11 ± 0.01
	Dry air	1.96		0.5409 ± 0.0047	3.81 ± 0.04	2.06 ± 0.02
SiO_2	Ambient Air	1.448	149.3	0.6890 ± 0.0040	4.23 ± 0.15	2.91 ± 0.10
	Dry air	1.446		0.7012 ± 0.0099	4.07 ± 0.25	2.85 ± 0.17

Table 8: experimental LIDTs ($LIDT_{exp}$) of HfO_2 end SiO_2 monolayers measured in ambient and dry air, at 0° AOI during the campaign at Lab B . Intrinsic LIDTs ($LIDT_{int}$) were estimated with EFI calculated from refractive indices measured in ambient and air environments.

Despite this analysis, a significant difference was nevertheless obtained experimentally between tests carried out in air and in vacuum. Table 2 reports higher $LIDT_{exp}$ in vacuum than in air, these results were obtained by both Lab C and Lab E. For hafnia coating, $LIDT_{int}$ are 1.42 and 1.34 J.cm^{-2} in air and 1.63 and 1.52 J.cm^{-2} in vacuum, from laboratories C and E, respectively. This means a difference of around 13% for the two labs.

e) Error budget: One can consider an exhaustive list of all sources of error leading to an approximate determination of the damage thresholds. However, the most important ones are arguably the following:

- Fluence is the most common quantity measured: The error on energy is only a few percent because the pyroelectric detectors are calibrated against a standard. Measuring the area of the beam is certainly one of the most delicate measurements. In a previous article comparing cameras, measurement plans, and correlations between different measurement means, it emerged that an absolute error of 10% is to be taken into account on this parameter [18]. Sozet [22] has also estimated an absolute error about 10% for laser damage tests carried out at 1053nm-0.7fs on the DERIC facility taking into account the errors on beam-energy measurement and on equivalent-area determination.

- Damage detection, even with the help of a microscope, is somewhat subjective. It is difficult to quantify its weight in the error budget. Sozet [23], by comparing two measurement procedures, reported a difference of 5% linked to the criterion for determining the threshold.
- Chorel [24] focused on the error in determining the intrinsic threshold, paying particular attention to the errors in the EFI based on uncertainties in the thicknesses and refractive indices of the layers. This makes it possible to give advice on reducing this uncertainty, for example by optimizing the angle of incidence of the tests. We can refer to the article as a whole for more information.
- Pulse duration is estimated from the autocorrelation trace. Again, an error of the order of 10% is to be considered. But beyond that, a strong relationship emerges between the damage threshold and the true intensity profile [13], the latter not being known and measured on a daily basis. Small differences in intensity profiles can result in large differences in thresholds. These differences must be taken into account on a case-by-case basis.
- Within the context of the analysis provided in this work, we have assumed that the damage threshold under exposure to sub-ps pulses is not dependent of the size of the damage testing beam spot. This is considered to be valid as damage initiation tests the fundamental limits of the material and is not dependent on the density of a defect distribution (damage is initiated by electric-field–induced volume breakdown [10]). However, this might not be entirely correct. This difference can arise from energy balance considerations, namely that damage requires not only the deposition of energy to create volume breakdown conditions but also the energy to generate the observed material modifications. It is the later component that may be sensitive to the area of the ablated volume (thus, the size of the damage testing beam). To the best of our knowledge, the potential role of this process in the measured damage threshold under exposure to sub-ps laser pulses has not been explored yet. However, there are publications that indicate a dependence of the ablation threshold of materials on the beam size [25, 26, 27]. Also, a recent work focused on the damage threshold in dielectric materials and coatings [28] seems to indicate (see Fig. 5 of [28]) that the damage threshold at pulse durations similar to those used in this work vary by up to about 15% for beam waists of 100 µm, 50 µm, and 30 µm. Therefore, the size of the damage testing beam may be another parameter that can have an impact in the measured damage threshold and may require additional study.

Thus, considering the analysis of the impact of all of these different contributors (they are summarized in Table 9 with the assumption that they are not correlated), it is appropriate to consider that differences around 20 % between tests carried out on different facilities can be reasonably obtained.

Contributor		Error bar (%)
1	calorimeter	2
2	Beam size estimation	5
3	Damage detection	5
4	Pulse duration estimation and dependence	10
5	Beam size dependence	15

Table 9: Synthesis of error margins for identified contributors (error budget). A quadratic summation provides an accuracy around 20% for the determination of fluences.

IV CONCLUSION – PERSPECTIVES

The round robin conducted by 5 independent laboratories on LIDT measurements of two dielectric monolayers in the short pulse regime at 1 micron and for 4 different experimental configurations showed significant differences. Deviations on average of around 21% were obtained greater than the absolute measurement uncertainties on the facilities estimated at least 10%. This is an unexpected and highly undesirable result. LIDT determination in this pulse-length regime should be straightforward and results should be comparable. However, an analysis of the various contributors involved in the

measurement of damage thresholds shows that differences of 20% are nevertheless plausible. The hypothesized principal mechanism to explain such deviations needs to be explored in future work to resolve this challenge in determining damage-threshold measurements in the short pulse regime. We suggest that it is of fundamental importance to pay increased attention to metrology:

- Accurate beam spatial profile measurement with special attention to the sensor noise determination in the case of a small beam on a large sensor window.
- The problem of nonlinear beam propagation which affects the experimental measurements, mainly the beam profile, has to be considered.
- Experimental conditions have to be perfectly known and controlled, as for example hygrometry and/or environment.
- Precise knowledge of the temporal intensity profile is also imperative.

Acknowledgements:

This material is based in part upon work supported by the Department of Energy National Nuclear Security Administration under Award Number DE-NA0003856, the University of Rochester, and the New York State Energy Research and Development Authority. This report was prepared as an account of work sponsored by an agency of the U.S. Government. Neither the U.S. Government nor any agency thereof, nor any of their employees, makes any warranty, express or implied, or assumes any legal liability or responsibility for the accuracy, completeness, or usefulness of any information, apparatus, product, or process disclosed, or represents that its use would not infringe privately owned rights. Reference herein to any specific commercial product, process, or service by trade name, trademark, manufacturer, or otherwise does not necessarily constitute or imply its endorsement, recommendation, or favoring by the U.S. Government or any agency thereof. The views and opinions of authors expressed herein do not necessarily state or reflect those of the U.S. Government or any agency thereof. This work was performed under the auspices of the U.S. Department of Energy (DOE) by Lawrence Livermore National Laboratory under Contract DE-AC52-07NA27344.

REFERENCES

[1] L. J. Waxer, D. N. Maywar, J. H. Kelly, T. J. Kessler, B. E. Kruschwitz, S. J. Loucks, R. L. McCrory, D. D. Meyerhofer, S. F. B. Morse, C. Stoeckl, and J. D. Zuegel, "High-energy petawatt capability for the OMEGA laser," Opt. Photonics News **16**(7), 30–36 (2005).

[2] N. Blanchot, G. Béhar, J. C. Chapuis, C. Chappuis, S. Chardavoine, J. F. Charrier, H. Coïc, C. Damiens-Dupont, J. Duthu, P. Garcia, J. P. Goossens, F. Granet, C. Grosset-Grange, P. Guerin, B. Hebrard, L. Hilsz, L. Lamaignere, T. Lacombe, E. Lavastre, T. Longhi, J. Luce, F. Macias, M. Mangeant, E. Mazataud, B. Minou, T. Morgaint, S. Noailles, J. Neauport, P. Patelli, E. Perrot-Minnot, C. Present, B. Remy, C. Rouyer, N. Santacreu, M. Sozet, D. Valla, and F. Laniesse, "1.15 PW-850 J compressed beam demonstration using the PETAL facility," Opt. Express **25**(15), 16957–16970 (2017).

[3] J. E. Heebner, R. L. Acree Jr., D. A. Alessi, A. I. Barnes, M. W. Bowers, D. F. Browning, T. S. Budge, S. Burns, L. S. Chang, K. S. Christensen, J. K. Crane, M. Dailey, G. V. Erbert, M. Fischer, M. Flegel, B. P. Golick, J. M. Halpin, M. Y. Hamamoto, M. R. Hermann, V. J. Hernandez, J. Honig, J. A. Jarboe, D. H. Kalantar, V. K. Kanz, K. M. Knittel, J. R. Lusk, W. A. Molander, V. R. Pacheu, M. Paul, L. J. Pelz, M. A. Prantil, M. C. Rushford, N. Schenkel, R. J. Sigurdsson, T. M. Spinka, M. G. Taranowski, P. J. Wegner, KaK.rl C. Wilhelmsen, J. Nan Wong, and S. T. Yang, "Injection laser system for Advanced Radiographic Capability using chirped pulse amplification on the National Ignition Facility", Applied Optics **58**, 8501 (2019).

[4] J. Néauport, E. Lavastre, G. Razé, G. Dupuy, N. Bonod, M. Balas, G. de Villele, J. Flamand, S. Kaladgew, and F. Desserouer, "Effect of electric field on laser induced damage threshold of multilayer dielectric gratings," Opt. Express **15**(19), 12508–12522 (2007).

[5] R. A. Negres, C. W. Carr, T. A. Laurence, K. Stanion, G. Guss, D. A. Cross, P. J. Wegner, and C. J. Stolz, "Laser-induced damage of intrinsic and extrinsic defects by picosecond pulses on multilayer dielectric coatings for petawatt-class lasers", Optical Engineering **56**, 011008 (2017).

[6] M. Chorel, T. Lanternier, E. Lavastre, N. Bonod, B. Bousquet, and J. Néauport, "Robust optimization of the laser induced damage threshold of dielectric mirrors for high power lasers", Optics Express **26**, 1176 (2018).

[7] B. C. Stuart, M. D. Feit, A. M. Rubenchik, B. W. Shore, and M. D. Perry, "Laser-induced damage in dielectrics with nanosecond to subpicosecond pulses," Phys. Rev. Lett. **74**(12), 2248–2251 (1995).

[8] M. Mero, J. Liu, W. Rudolph, D. Ristau and K. Starke, "Scaling laws of femtosecond laser pulse induced breakdown in oxide films", Phys. Rev. B. **71**, 115109 (2005).

[9] B. Mangote, L. Gallais, M. Zerrad, F. Lemarchand, L. H. Gao, M. Commandré, and M. Lequime, "A high accuracy femto-/picosecond laser damage test facility dedicated to the study of optical thin films", Review of Scientific Instruments **83**, 013109 (2012).

[10] A. A. Kozlov, J. C. Lambropoulos, J. B. Oliver, B. N. Hoffman, and S. G. Demos, "Mechanisms of picoseconds laser-induced damage in common multilayer dielectric coatings," Sci. Rep. **9**(1), 607 (2019).

[11] B. Rethfeld, O. Brenk, N. Medvedev, H. Krutsch, and D. H. H. Hoffman, "Interaction of dielectrics with femtosecond laser pulses: application of kinetic approach and multiple rate equation", Appl. Phys. A **101**, 19 (2010).

[12] L. Gallais, D.-B. Douti, M. Commandre, G. Bataviciute , E. Pupka, M. Sciuka, L. Smalakys, V. Sirutkaitis, and A. Melninkaitis, "Wavelength dependence of femtosecond laser-induced damage threshold of optical materials", Journal of Applied Physics **117**, 223103 (2015).

[13] A. Olle, J. Luce, N. Roquin, C. Rouyer, M. Sozet, L. Gallais, and L. Lamaignère, "Implications of laser beam metrology on laser damage temporal scaling law for dielectric materials in the picosecond regime", Rev. Sci. Instr. **90**, 073001 (2019). doi: 10.1063/1.5094774

[14] ISO Standard Nos. 21254-1─21254-4 (2011).

[15] R. Trebino, "Frequency-Resolved Optical Gating: The Measurement of Ultrashort Laser Pulses" (Kluwer Academic, 2000).

[16] D. Bigourd, J. Luce, E. Mazataud, E. Hugonnot, and C. Rouyer, "Direct spectral phase measurement with spectral interferometry resolved in time extra dimensional" Rev. Sci. Instrum. **81**, 053105 (2010).

[17] K. Gaudfrin, J. Lopez, K. Mishchik, L. Gemini, R. Kling, and G. Duchateau, “Fused silica ablation by double femtosecond laser pulses: influence of polarization state”, Optics Express **28**, 15189 (2020).
[18] L. Lamaignère, M. Balas, R. Courchinoux, T. Donval, J. C. Poncetta, S. Reyné, B. Bertussi, and H. Bercegol, “Parametric study of laser-induced surface damage density measurements: Toward reproducibility”, J. Appl. Phys. **107**, 023105 (2010).
[19] E. T. J. Nibbering, G. Grillon, M. A. Franco, B. S. Prade and A. Mysyrowicz, "Determination of the inertial contribution to the nonlinear refractive index of air, N_2 and O_2 by use of unfocused high-intensity femtosecond laser pulses", J. Opt. Soc. Am. B **14**, 650-660 (1997).
[20] D. Villate, N. Blanchot, and C. Rouyer, “Beam breakup integral measurement on high-power laser chains”, Optics Letters **32**, 524-526 (2007).
[21] J. B. Oliver, S. Papernov, A. W. Schmid, and J. C. Lambropoulos "Optimization of laser-damage resistance of evaporated hafnia films at 351nm", Proc. SPIE **7132**, 71320J (2008).
[22] M. Sozet, J. Néauport, E. Lavastre, N. Roquin, L. Gallais, and L. Lamaignère, “Laser damage density measurement of optical components in the sub-picosecond regime”, Optics Letters **40**, 2091 (2015).
[23] M. Sozet, J. Néauport, E. Lavastre, N. Roquin, L. Gallais, and L. Lamaignère, “Assessment of mono-shot measurement as a fast and accurate determination of the laser-induced damage threshold in the sub-picosecond regime”, Optics Lett. **41**, 804 (2016).
[24] M. Chorel, S. Papernov, A. A. Kozlov, B. N. Hoffman, J. B. Oliver, S. G. Demos, T. Lanternier, É. Lavastre, L. Lamaignère, N. Roquin, B. Bousquet, N. Bonod, and J. Néauport, “Influence of absorption-edge properties on subpicosecond intrinsic laser-damage threshold at 1053 nm in hafnia and silica monolayers”, Optics Express **27**, 16922 (2019).
[25] B. M. Kim, M. D. Feit, A. M. Rubenchik, E. J. Joslin, J.Eichler, P. C. Stoller and L. B. Da Silva, “Effects of high repetition rate and beam size on hard tissue damage due to subpicosecond laser pulses”, Appl. Phys. Lett. **76**, 4001-4003 (2000).
[26] S. Martin, A. Hertwig, M. Lenznerj. Kruger, W. Kautek, “Spot-size dependence of the ablation threshold in dielectrics for femtosecond laser pulses” Appl. Phys. A **77**, 883–884 (2003).
[27] A. Hertwig, S. Martin, J. Kruger, W. Kautek “Interaction area dependence of the ablation threshold of ion-doped glass”, Thin Solid Films **453 –454**, 527–530 (2004).
[28] T. A. Laurence, R. A. Negres, S. Ly, N. Shen, C. W. Carr, D. A. Alessi, A. Rigatti, J. D. Bude, “The role of defects in laser-induced modifications of silica coatings and fused silica using picosecond pulses at 1053 nm: II. Scaling laws and the density of precursors”, Opt. Express **25**, 15381- 15401 (2018).